FUDMA Journal of Sciences (FJS)
ISSN online: 2616-1370
ISSN print: 2645 - 2944
Vol. 10 No. 8, April, 2026, pp 392 – 400
DOI: https://doi.org/10.33003/fjs-2026-1008-5079

Computational Thermal Analysis of AISI 1018 Low-Carbon Steel during Gas Tungsten Arc Welding

***[1]Ejiroghene Kelly Orhorhoro and [2]Oghenekevwe Oghoghorie**

[1]Department of Mechanical Engineering, College of Engineering, Igbinedion University, Okada, Edo State, Nigeria.
[2]Department of Mechanical Engineering, Faculty of Engineering, Benson Idahosa University, Benin City, Edo State, Nigeria.

*Corresponding authors' email: ejiroghene.orhorhoro@iuokada.edu.ng

ABSTRACT
The thermal behaviour of AISI 1018 low-carbon steel during Gas Tungsten Arc Welding (GTAW) is thoroughly investigated computationally in this work utilising computational fluid dynamics and finite volume methods. The study assesses how heat input affects the welded region's temperature distribution, thermal conductivity, dynamic viscosity, specific heat capacity, weld pool behaviour, and heat flux properties. To replicate actual welding conditions, a three dimensional transient thermal model with temperature dependent thermophysical characteristics and a Gaussian moving heat source was created. The findings show that GTAW offers localised heating, controlled thermal penetration, reduced heat affected zone, and improved weld quality. The study provides important insight for optimising GTAW parameters and improving thermal management in steel fabrication industries. The simulation results showed peak temperatures exceeding 4000 K within the fusion zone, confirming stable weld pool formation and effective heat penetration. Thermal conductivity and dynamic viscosity decreased with increasing temperature, while specific heat capacity increased significantly, influencing heat diffusion and molten metal flow. As the temperature rose, specific heat capacity dramatically increased, affecting heat diffusion and the flow of molten metal, but thermal conductivity and dynamic viscosity decreased. The results show that GTAW offers enhanced weld quality, reduced heat affected zone, regulated thermal penetration, and localised heating. The study offers important information for enhancing heat management in steel manufacturing businesses and optimising GTAW parameters.

Keywords: Gas Tungsten Arc Welding, AISI 1018 Low-Carbon Steel, Thermal Behaviour, Computational Fluid Dynamics, Finite Volume Method, Weld Pool Dynamics

INTRODUCTION

Welding is still one of the most important manufacturing and construction methods used in modern engineering fields because it can produce strong, durable, and reliable joints in metallic constructions. Because of its superior weld quality, excellent arc stability, minimal spatter generation, and capacity to produce defect free joints with high dimensional precision, Gas Tungsten Arc Welding (GTAW), also known as Tungsten Inert Gas (TIG) welding, has gained significant industrial acceptance among the various welding techniques available (Ahmad *et al.*, 2022; Ali *et al.*, 2023). Weld integrity and metallurgical quality are vital in the aerospace, automotive, marine, petrochemical, structural, and power generation industries, where GTAW is widely used (Arora *et al.*, 2022; Patel *et al.*, 2022). One of the most important factors influencing weld quality, residual stress production, microstructural development, heat affected zone (HAZ) properties, and mechanical performance of welded structures is the thermal behaviour of materials during welding (Chen *et al.*, 2022; Babu *et al.*, 2023). Localised temperatures high enough to melt the base metal and filler material are produced during GTAW by an intense electric arc created between a non-consumable tungsten electrode and the workpiece. The resulting thermal cycles produce complex heat transfer phenomena involving conduction, convection, radiation, melting, solidification, and fluid flow within the molten weld pool (Elangovan & Balasubramanian, 2022; Farahani *et al.*, 2023). These thermal interactions have a significant impact on the final properties of the welded joint (Das *et al.*, 2023). Complex heat transmission phenomena including conduction, convection, radiation, melting, solidification, and fluid flow inside the molten weld pool are produced by the ensuing thermal cycles (Elangovan & Balasubramanian, 2022; Farahani *et al.*, 2023). The ultimate characteristics of the welded joint are significantly impacted by these thermal interactions (Das *et al.*, 2023).

Moreover, as a result of their good ductility, moderate strength, excellent machinability, low cost, and superior weldability, low carbon steels especially AISI 1018 steel, which normally contains about 0.18 weight percent carbon, which lessens the susceptibility to brittle phase formation and weld cracking during thermal processing are used extensively in the fabrication of machine components, pressure vessels, pipelines, automotive frames, shafts, structural supports, and industrial equipment (Yadav & Chauhan, 2022). The usual carbon content of AISI 1018 steel is about 0.18 weight percent, which lessens the material's vulnerability to weld cracking and brittle phase formation during thermal processing (Yadav & Chauhan, 2022). Because of these characteristics, the material is widely used in the production of industrial equipment, automotive frames, shafts, pressure vessels, pipelines, machine components, and structural supports. Even though AISI 1018 steel has a favourable weldability, the material still undergoes significant thermal and metallurgical changes during GTAW operations (Ghosh & DebRoy, 2022; Natarajan & Ravi, 2022). The concentrated heat source associated with GTAW generates rapid heating and cooling cycles that cause non-uniform thermal gradients across the weldment, which result in residual stresses, thermal distortion, grain coarsening, and localised phase transformations within the weld metal and heat affected zone. Excessive thermal accumulation may also have a negative effect on the mechanical strength, fatigue resistance, dimensional accuracy, and corrosion performance of welded

components (Ramesh et al., 2022; Sharma & Singh, 2023). Rapid heating and cooling cycles caused by the focused heat source connected to GTAW result in uneven temperature gradients across the weldment. Within the weld metal and heat-affected zone, these gradients cause residual stresses, thermal deformation, grain coarsening, and localised phase transitions. The mechanical strength, fatigue resistance, dimensional correctness, and corrosion performance of welded components can all be negatively impacted by excessive thermal accumulation (Ramesh *et al.*, 2022; Sharma & Singh, 2023). Because of the high temperatures and quick transient phenomena involved in welding, experimental investigations alone are frequently costly, time consuming, and challenging to conduct. As a result, numerical simulation and computational thermal analysis have emerged as potent alternatives for predicting weld pool dynamics, temperature distribution, heat flow behaviour, and metallurgical transformations in welded materials (Siva & Balaji, 2022; Tiwari & Dubey, 2022; Sun *et al.*, 2023). Because welding involves severe temperatures and fast transient events, doing experimental research alone is frequently costly, time consuming, and challenging. As a result, weld pool dynamics, temperature distribution, heat flow behaviour, and metallurgical transformations in welded materials can now be predicted using numerical simulation and computational thermal analysis (Siva & Balaji, 2022; Tiwari & Dubey, 2022; Sun *et al.*, 2023). Because they offer a thorough understanding of the thermal-fluid interactions within the weld pool, computational fluid dynamics (CFD) and finite volume approaches are being utilised more frequently to simulate welding processes (Hassan *et al.*, 2022; Gupta et al., 2023). Under various welding settings, transient temperature fields, heat flux distribution, molten metal convection, cooling rates, and phase transition behaviour may all be predicted using numerical models (He et al., 2023; Oladimeji & Akinlabi, 2023). These methods increase process optimisation and weld design accuracy while drastically lowering experimental expenses.

Recent studies have shown that heat source characteristics, welding speed, current intensity, arc efficiency, and material thermo-physical properties strongly influence thermal distribution and weld penetration during GTAW (Kannan & Murugan, 2023). They have also shown that temperature-dependent properties like thermal conductivity, specific heat capacity, viscosity, and electrical resistivity significantly affect molten pool behaviour and thermal diffusion mechanisms (Li *et al.*, 2023; Wang *et al.*, 2023). According to recent research, thermal distribution and weld penetration during GTAW are significantly influenced by heat source characteristics, welding speed, current intensity, arc efficiency, and material thermo-physical properties (Kannan & Murugan, 2023). Additionally, studies have demonstrated that temperature-dependent characteristics including electrical resistivity, viscosity, thermal conductivity, and specific heat capacity have a major impact on the behaviour of molten pools and thermal diffusion mechanisms (Li *et al.*, 2023; Wang *et al.*, 2023). Additionally, advances in numerical welding simulation have made it possible to predict weld pool morphology and heat-affected zone development more accurately (Mahmood *et al.*, 2022; Zhang *et al.*, 2023). Phase transformation analysis, moving heat source formulations, and transient heat transfer models have improved understanding of thermal responses in low carbon steels under high energy welding conditions (Mohanty & Biswas, 2023). Nevertheless, few studies have used detailed computational methods to thoroughly investigate the coupled thermal behaviour, heat flux characteristics, and temperature-dependent material responses of AISI 1018 low carbon steel during GTAW. Understanding of thermal responses in low carbon steels under high energy welding settings has increased with the use of phase transformation analysis, moving heat source formulations, and transient heat transfer models (Mohanty & Biswas, 2023). Nevertheless, despite these advancements, few research have used computational techniques to thoroughly investigate the coupled thermal behaviour, heat flow characteristics, and temperature-dependent material reactions of AISI 1018 low carbon steel during GTAW. The current study focuses on the thermal behaviour of AISI 1018 low carbon steel subjected to Gas Tungsten Arc Welding using computational thermal analysis. Thermal conductivity plays a crucial role in controlling heat diffusion through the workpiece, specific heat capacity determines the material's ability to absorb thermal energy during heating, dynamic viscosity influences molten metal flow and weld pool stability, and radiative and convective heat transfer mechanisms govern cooling behaviour. Therefore, establishing stable weld formation, reducing flaws, and enhancing structural reliability depend on accurate modelling of these thermo-physical interactions. In order to simulate transient heat transfer during welding, a three-dimensional computational domain was developed and discretised using finite volume techniques. Temperature dependent thermo-physical properties were incorporated into the model to improve simulation realism and predictive capability. The welding arc was represented using a concentrated moving heat source, and convective and radiative heat losses were included to accurately capture thermal dissipation mechanisms. The study also evaluates temperature evolution within the weld region and analyses the influence of heat input and temperature variation. Additionally, the study assesses the evolution of temperature inside the weld zone and examines how thermal gradients affect melting behaviour and weld stability. The study's findings may also support future developments in automated welding systems, computational welding optimisation, and advanced thermal management strategies for steel fabrication industries. The significance of this research lies in its contribution to improving understanding of thermal transport phenomena in GTAW of low carbon steels. It is anticipated that the study's findings would yield useful information for optimising GTAW process parameters, promoting weld pool stability, reducing thermal distortion and residual stresses, improving weld penetration and fusion quality, and increasing industrial welding efficiency. Future advancements in automated welding systems, computational welding optimisation, and sophisticated heat management techniques for the steel fabrication sector may also benefit from the findings.

MATERIALS AND METHODS

Materials

AISI 1018 low carbon steel was selected for this study because of its superior weldability, moderate mechanical strength, low carbon content, and numerous industrial applications in pipelines, automotive components, pressure vessels, and structural construction. Its temperature-dependent thermo-physical and mechanical properties were used to accurately simulate the thermal response during Gas Tungsten Arc Welding (GTAW). In order to precisely replicate the thermal reaction during GTAW, the material's temperature-dependent thermo-physical and mechanical properties were modelled. The ultimate tensile strength of 440 MPa, yield strength of 370 MPa, modulus of elasticity of 205 GPa, Poisson's ratio of 0.29, and temperature-dependent

thermal conductivity were among the mechanical characteristics of AISI 1018 steel used in the simulation, as indicated in Table 1. To increase computational accuracy, thermophysical characteristics such density, electrical resistivity, thermal conductivity, dynamic viscosity, and specific heat capacity were added as temperature-dependent variables.

Table 1: Mechanical Properties of AISI 1018 Steel used in the Numerical Model

Mechanical Properties	Metric	Imperial
Hardness, Brinell	126	126
Hardness, Knoop (Converted from Brinell hardness)	145	145
Hardness, Rockwell B (Converted from Brinell hardness)	71	71
Hardness, Vickers (Converted from Brinell hardness)	131	131
Tensile Strength, Ultimate	440 MPa	63800 psi
Tensile Strength, Yield	370 MPa	53700 psi
Elongation at Break (In 50 mm)	15.0 %	15.0 %
Reduction of Area	40.0 %	40.0 %
Modulus of Elasticity (Typical for steel)	205 GPa	29700 ksi
Bulk Modulus (Typical for steel)	140 GPa	20300 ksi
Poissons Ratio (Typical for Steel)	0.290	0.290
Machinability (Based on AISI 1212 steel. as 100% machinability)	70 %	70 %
Shear Modulus (Typical for steel)	80.0 GPa	11600 ksi

Computational Domain and Geometry Development

Using computational fluid dynamics (CFD) and finite volume techniques, a three-dimensional computational domain representing the weld plate and surrounding thermal environment was created. The domain dimensions were carefully chosen to minimise boundary effects and ensure accurate heat transfer predictions around the weld region. Table 2 shows the computational dimensions adopted for the simulation. The GTAW heat source was positioned centrally along the welding path to ensure uniform thermal distribution and symmetrical heat propagation during analysis. In order to reduce boundary effects and guarantee precise heat transfer predictions surrounding the weld site, the domain dimensions were carefully chosen. Table 2 displays the computational dimensions used for the simulation. The molten pool, nearby base metal, and heat affected zone (HAZ) were all adequately covered spatially by these dimensions. To guarantee consistent thermal distribution and symmetrical heat propagation throughout analysis, the GTAW heat source was placed in the middle of the welding path.

Table 2: Size Computational Domain

X min	-0.060 m
X max	6.000e-005 m
Y min	-1.100e-005 m
Y max	0.011 m
Z min	-7.000e-005 m
Z max	0.070 m

Mesh Generation

To increase numerical stability and thermal gradient prediction accuracy, the computational geometry was discretised using a structured finite volume mesh. Mesh independence was taken into account during discretisation to guarantee dependable convergence and reduce computational errors. The mesh configuration that was chosen included:

i. 78 cells along the X-axis,
ii. 14 cells along the Y-axis, and
iii. 90 cells along the Z-axis.

Because of the quick phase change and severe heat gradients in the weld pool and fusion zone, the mesh density was refined in these areas. In order to lower computational costs without sacrificing solution accuracy, coarser mesh elements were applied further from the heat source. The mesh that was created allowed for precise prediction of:

i. Distribution of temperature,
ii. Variation in heat flux,
ii. Features of fluid flow,
iii. Melting behaviour, and
iv. Thermal diffusion in the weldment.

Governing Equations

The basic conservation equations for mass, momentum, and energy were used to predict the thermal and fluid flow behaviour during GTAW.

Continuity Equation

The conservation of mass for incompressible fluid flow within the molten weld pool is expressed as:

$$\frac{\partial \rho}{\partial t} + \nabla \cdot (\rho \vec{V}) = 0 \quad (1)$$

Where ρ represents fluid density, $\vec{V}$ denotes velocity vector, and t represents time.

Momentum Equation

The momentum conservation equation governing molten metal flow inside the weld pool is given by:

$$\rho\left(\frac{\partial \vec{V}}{\partial t} + \vec{V} \cdot \nabla \vec{V}\right) = -\nabla P + \mu \nabla^2 \vec{V} + \rho g \quad (2)$$

This equation characterises the convective flow behaviour caused by thermal gradients and arc-driven fluid motion within the molten weld pool, where P represents pressure, μ is dynamic viscosity, and g denotes gravity acceleration. The convective flow behaviour in the molten weld pool caused by

heat gradients and arc-driven fluid motion is described by this equation.

Energy Equation

Heat transfer during welding was governed by the transient energy equation:

$$\rho C_p \frac{\partial T}{\partial t} = k\nabla^2 T + Q \quad (3)$$

Where Q stands for internal heat generation from the welding arc, Cp is specific heat capacity, T is temperature, and K is thermal conductivity. The formula takes into consideration the material's internal thermal energy generation, heat accumulation, and conductive heat transport.

Heat Source Modeling

A moving focused heat source with Gaussian heat distribution properties was used to represent the GTAW arc. It was anticipated that the heat input produced by the tungsten electrode was evenly dispersed over the weld surface. Equation (4) was used to determine the total heat input.

$$Q = \eta VI \quad (4)$$

Where I stands for welding current, V for arc voltage, Q for welding heat input, and η for welding efficiency. Equation (5) depicts the Gaussian heat flux distribution.

$$q(r) = \frac{3Q}{\pi r_0^2}\exp(-\frac{3r^2}{r_0^2}) \quad (5)$$

Where $q(r)$is radial heat flux, $r_0$is effective arc radius, and r is radial distance from arc center. This model accurately represented the concentrated thermal intensity produced by the GTAW arc.

Boundary Conditions

To precisely replicate welding circumstances, the proper thermal and flow boundary conditions were used.

Pressure Boundary

To enable vortex-induced flow circulation within the weld region, environmental pressure conditions were applied at the inlet and outflow boundaries. The ratios of inflow to exit flow were roughly:

i. 0.762002
ii. 0.769804

Realistic molten metal convection and thermal circulation during welding were replicated under these circumstances.

Thermal Boundary Conditions

The simulation took into account both convective and radiative heat losses from the workpiece surface. The Stefan-Boltzmann equation was used to represent heat dissipation through radiation: The Stefan-Boltzmann equation was used to simulate heat dissipation by radiation:

$$q_r = \varepsilon\sigma(T^4 - T_\infty^4) \quad (6)$$

Where ε is emissivity, σ is Stefan–Boltzmann constant, and T_∞ is ambient temperature. Natural convection heat transfer was modeled as:

$$q_c = h(T - T_\infty) \quad (7)$$

Where h is convective heat transfer coefficient;

Phase Change and Melting Analysis

An enthalpy-based phase transformation model was used to incorporate the melting behaviour of AISI 1018 steel during GTAW. The simulation tracked the solid-liquid transition, fusion zone evolution, temperature-dependent resistivity, and weld pool expansion. Temperature-dependent resistivity, weld pool expansion, solid-liquid transition, and fusion zone evolution were all tracked by the simulation.

Solution Procedure

A transient finite volume solver was used to carry out the numerical simulation. The simulation monitored the average fluid temperature, mean radiant temperature, heat flux, maximum solid temperature, and minimum solid temperature. Temperature-dependent material properties were updated continuously throughout the simulation to improve predictive accuracy. Iterative calculations were carried out until convergence criteria for temperature, heat flux, and fluid flow variables were satisfied. These criteria included the average temperature stabilisation, heat flux convergence, maximum temperature consistency, and residual reduction below acceptable tolerance levels. Temperature, heat flux, and fluid flow variables were calculated iteratively until the convergence requirements were met. Average temperature stabilisation, heat flux convergence, maximum temperature consistency, and residual reduction below allowable tolerance limits were among the convergence criteria. Average fluid temperature, mean radiant temperature, heat flow, maximum solid temperature, and minimum solid temperature were all tracked by the simulation. To increase prediction accuracy, temperature-dependent material properties were updated continually during the simulation.

RESULTS AND DISCUSSION

The intricate relationship between heat transport, material qualities, melting characteristics, and thermal energy distribution within the weld zone is illustrated by the thermal behaviour of AISI 1018 low carbon steel during Gas Tungsten Arc Welding (GTAW). Significant thermal gradients, high peak temperatures, and temperature-dependent changes in thermo-physical characteristics were found in the simulation findings. These factors have a substantial impact on structural integrity, metallurgical transformations, and weld quality.

Thermal Distribution Behaviour

The findings of the thermal simulation for the GTAW of AISI 1018 low-carbon steel show that heat input and thermal expansion have a major impact on the material's overall structural response, heat-affected zone (HAZ), and weld thermal field. The study's simulation graphics demonstrate gradual changes in the temperature distribution that correlate to various weld lengths and thermal expansion coefficients. The temperature contour plots show that the GTAW heat source is directly applied along the weld bead region, where the highest temperatures are concentrated (Figure 1).

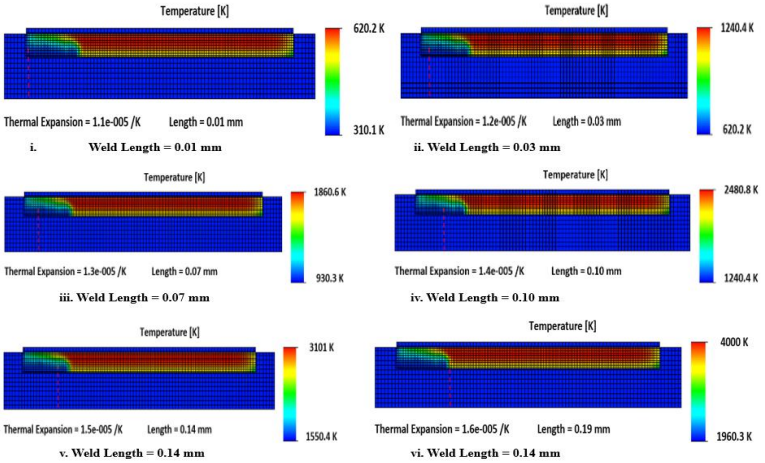

Figure 1: Thermal Simulation Results for the Gas Tungsten Arc Welding (GTAW) of AISI 1018 Low-Carbon Steel

The molten or almost molten weld pool is shown by the red and orange regions, and the comparatively cooler base metal parts are indicated by the blue regions. Because of the extremely concentrated and localised arc heat source, this phenomenon is typical of GTAW processes. Maximum temperature ranges between around 1240 K and 4000 K are revealed by the simulations. The weld zone suffers strong thermal concentration at the peak temperature condition of 4000 K, suggesting significant heat penetration into the substrate. These high temperatures are enough to cause partial melting close to the fusion boundaries and complete melting of the filler region. One of the main benefits of GTAW is the narrow heat-affected zone seen in the contour plots, which minimises excessive metallurgical degradation and maintains the mechanical properties of the surrounding material. The simulations also show thermal expansion coefficients ranging from $1.2 \times 10^{-5}/K$ to $1.6 \times 10^{-5}/K$. A steep thermal gradient is seen moving away from the weld centerline, confirming rapid heat dissipation into the surrounding parent metal through thermal conduction. This gradient verifies that thermal conduction causes rapid heat dissipation into the surrounding parent metal. One of the main benefits of GTAW is the limited heat-affected zone seen in the contour plots, which reduces excessive metallurgical degradation and maintains the mechanical characteristics of the surrounding material. Additionally, the corresponding weld expansion length increases from roughly 0.03 mm to 0.19 mm as the thermal expansion coefficient increases, confirming the direct relationship between thermal loading and material deformation. The welded component experiences significant dimensional changes during heating, as indicated by the increase in thermal expansion with rising temperature (Zhang *et al.*, 2023). If these expansions are not properly controlled, they can result in residual stresses and post-weld distortions after cooling (Yadav & Chauhan, 2022). This behaviour demonstrates that thermal loading and material deformation are directly related (Zhang *et al.*, 2023). The welded component experiences substantial dimensional changes during heating, as seen by the increase in thermal expansion with temperature. After cooling, these expansions may result in residual stresses and post-weld distortions if improperly managed (Yadav & Chauhan, 2022).

For AISI 1018 low-carbon steel, the HAZ may show grain coarsening near the fusion boundary, reduced hardness in overheated regions, residual tensile stresses after cooling, and localised thermal softening (Natarajan, & Ravi, 2022). However, because GTAW provides controlled heat input, the HAZ remains relatively narrow and uniform compared with other fusion welding techniques like Shielded Metal Arc Welding (SMAW) or Submerged Arc Welding (SAW) (Mahmood *et al.*, 2022). The simulations suggest relatively stable heat propagation along the weld bead. High temperatures below the melting point cause microstructural changes in the HAZ without any melting. The HAZ for AISI 1018 low-carbon steel may show localised thermal softening, lower hardness in overheated areas, residual tensile stresses after cooling, and grain coarsening close to the fusion boundary (Natarajan, & Ravi, 2022). In contrast to other fusion welding methods like Shielded Metal Arc Welding (SMAW) or Submerged Arc Welding (SAW), the HAZ is still comparatively homogeneous and narrow since GTAW offers controlled heat input (Mahmood *et al.*, 2022). According to the models, heat propagation along the weld bead is comparatively stable. The absence of irregular thermal hotspots or abrupt discontinuities suggests good weld penetration, uniform fusion characteristics, reduced risk of thermal cracking, and improved weld quality (Patel *et al.*, 2022; Oladimeji & Akinlabi, 2023). However, at very high temperatures approaching 4000 K, there is a chance of excessive evaporation, oxidation, or metallurgical instability if shielding conditions are insufficient. Similarly, the gradual increase in expansion length from 0.03 mm to 0.19 mm indicates the development of internal restraint within the structure because the heated weld zone expands and contracts more quickly than the surrounding base metal. Additionally, good weld penetration, homogeneous fusion properties, a lower risk of thermal cracking, and higher weld quality are implied by the lack of irregular thermal hotspots or abrupt discontinuities (Patel *et al.*, 2022; Oladimeji & Akinlabi, 2023). However, if shielding conditions are insufficient, severe evaporation, oxidation, or metallurgical instability may occur at very high temperatures near 4000 K. The possibility of residual stress building while cooling is also indicated by the expansion length's gradual increase from 0.03 mm to 0.19 mm. internal restraint occurs within the structure because the hot weld zone expands and compresses faster than the surrounding base metal. However, from a mechanical engineering standpoint, the simulation effectively illustrates the thermal behaviour of AISI 1018 steel under GTAW conditions. The results confirm that GTAW offers highly localised heating, controlled thermal penetration, reduced HAZ width, improved weld precision, and lower distortion tendency compared with conventional arc welding methods. Overall, the simulation results show that the thermal response

of AISI 1018 low-carbon steel during GTAW is strongly dependent on heat input and thermal expansion behaviour. The simulation effectively illustrates the thermal behaviour of AISI 1018 steel under GTAW conditions from the standpoint of mechanical engineering. The findings verify that, in comparison to traditional arc welding techniques, GTAW offers highly localised heating, regulated thermal penetration, decreased HAZ width, enhanced weld precision, and a lower distortion propensity. Overall, the simulation findings show that heat input and thermal expansion behaviour have a significant impact on the thermal response of AISI 1018 low-carbon steel during GTAW. The results further confirm that GTAW is still an effective welding technique for low-carbon steel applications requiring high precision, controlled heat input, superior weld quality, and minimal metallurgical damage. The weld region experiences extremely high localised temperatures, while the surrounding material effectively dissipates heat. Increasing thermal expansion coefficients produce larger dimensional changes, which may contribute to residual stresses and distortion after cooling. Larger dimensional changes are produced by increasing thermal expansion coefficients, which could lead to distortion and residual strains after cooling. The findings further demonstrate that GTAW is still a successful welding method for low-carbon steel applications that need for excellent weld quality, controlled heat input, high precision, and little metallurgical damage.

Influence of Thermal Conductivity

The thermal conductivity values decreased progressively with increasing temperature, from approximately 0.2065 W/(m·K) at 180 K to 0.1150 W/(m·K) at 410 K as shown in Figure 2. This inverse relationship indicates that AISI 1018 steel becomes less efficient at conducting heat as temperature rises. The reduction in thermal conductivity has several important implications (Das *et al.*, 2023; Kannan, T., & Murugan, 2023):

i. Heat becomes increasingly concentrated around the weld zone.
ii. Thermal diffusion into the surrounding base material decreases.
iii. Localized overheating becomes more pronounced.
iv. Weld penetration and fusion efficiency increase.

The observed thermal behaviour is consistent with classical heat transfer theory for steels, where lattice vibrations and electron scattering increase at elevated temperatures, thereby reducing conductive heat transport efficiency (Natarajan & Ravi, 2022; Sun *et al.*, 2023). As conductivity decreases, the heat supplied by the GTAW arc remains confined within a smaller region, promoting deeper weld penetration and larger molten pools; however, excessive heat concentration may also promote thermal distortion, grain coarsening, and residual stress development. Excessive heat concentration, however, may also encourage the development of residual stress, grain coarsening, and thermal distortion. The observed thermal behaviour is consistent with the traditional heat transfer hypothesis for steels, which states that conductive heat transport efficiency decreases at higher temperatures due to an increase in lattice vibrations and electron scattering.

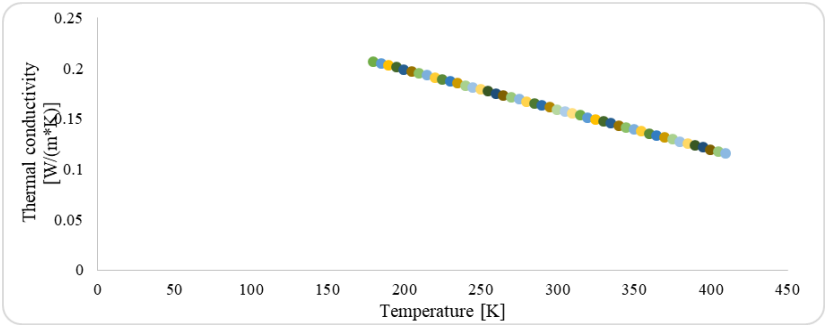

Figure 2: Evaluation of the Effect of Thermal Conductivity

Dynamic Viscosity Behaviour

The dynamic viscosity values decreased continuously with increasing temperature, ranging from approximately 1.9441×10^{-3} Pa.s at higher temperatures to lower temperatures at 1.3938×10^{-4} Pa.s as shown in Figure 3. This behaviour is predicted as the molten metals intermolecular cohesiveness is weakened by increasing heat energy, making fluid motion simpler (Natarajan & Ravi, 2022).

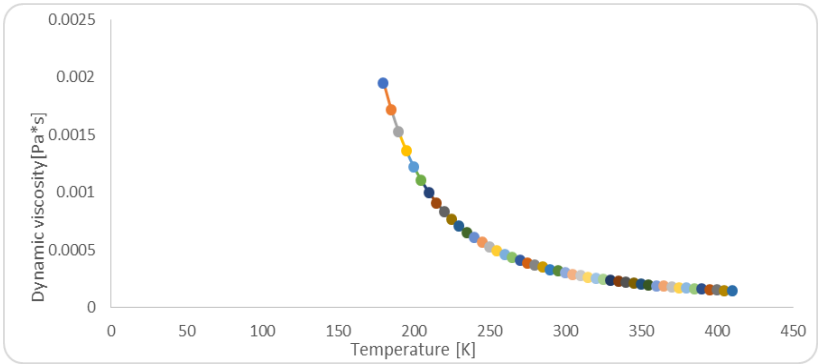

Figure 3. Analysis of Effect Dynamic Viscosity

The gradual decrease in viscosity confirms stable thermal softening behaviour of the material under GTAW conditions, and improved fluidity is especially helpful in achieving uniform weld formation and minimising porosity. Lower viscosity at elevated temperatures contributes to improved molten metal flow, better weld bead spreading, increased weld penetration, and enhanced impurity redistribution. However, excessively low viscosity may also cause instability in the molten pool, leading to defects like undercutting, excessive spatter, or irregular bead morphology. Improved molten metal flow, greater weld bead spreading, more weld penetration, and improved impurity redistribution are all facilitated by the decreased viscosity at higher temperatures. But too little viscosity can also make the molten pool unstable, which can result in flaws like undercutting, excessive spatter, or uneven bead morphology. The material's stable thermal softening behaviour under GTAW conditions is confirmed by the progressive decrease in viscosity. In order to minimise porosity and achieve uniform weld formation, improved fluidity is especially helpful.

Specific Heat Capacity Behaviour

The specific heat capacity (Cp) increased substantially with temperature, rising from approximately 2013.6 J/(kg·K) at 180 K to about 2723.9 J/(kg·K) at 410 K as shown in Figure 4.

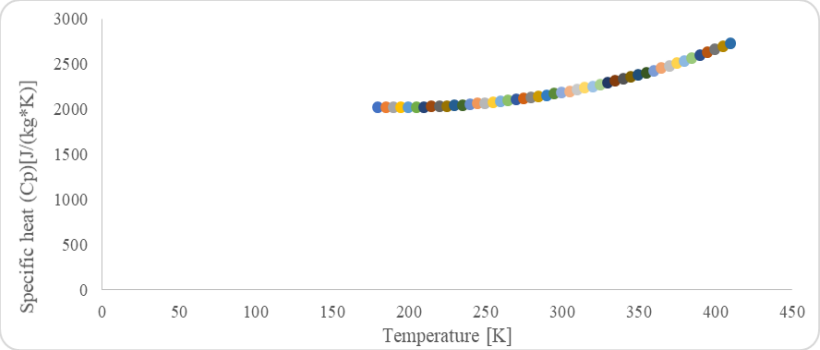

Figure 4: Evaluation of Specific Heat

Higher specific heat capacity at elevated temperatures influences welding behaviour in a number of ways, including increased energy input needed to sustain melting, improved thermal stability of the weld pool, a slight decrease in cooling rates, and an increase in heat retention within the weld region. This behaviour can be attributed to increased atomic vibrations and energy absorption mechanisms within the material. This capacity to store thermal energy affects the pace of solidification following arc passage and helps maintain molten conditions during welding. In the fusion zone and HAZ, slower cooling may encourage grain development, which could decrease hardness while increasing ductility. Improved thermal buffering capacity at higher temperatures, which helps lessen sudden thermal shocks during welding, is also suggested by the observed rise in Cp.

Mesh and Computational Domain Effects

The mesh discretisation and computational domain dimensions have a major impact on the accuracy of the solution. For capturing heat gradients and weld pool dynamics, the mesh configuration of 78 cells in the X-direction, 14 cells in the Y-direction, and 90 cells in the Z-direction offered sufficient spatial resolution. Improved prediction of heat flow along the welding route and depth penetration was made possible by the comparatively finer mesh in the X and Z dimensions. Because of the highly steep temperature gradients near the arc in GTAW simulations, accurate mesh discretisation is crucial. Numerical stability and dependable computational outcomes are indicated by the convergence values for the thermal parameters. The solution may have attained acceptable convergence levels if the average and maximum temperatures have small delta values.

CONCLUSION

This study effectively used numerical and thermo-fluid analytic tools to present a computational investigation into the thermal behaviour of AISI 1018 Low-Carbon Steel during Gas Tungsten Arc Welding. The simulation results showed that the welding technique produces peak temperatures high enough for full melting and stable weld pool formation by concentrating thermal energy inside the fusion region. The investigation showed that the localised Gaussian heat source and the thermo-physical properties of the material strongly influence the temperature distribution within the weldment. The narrow heat affected zone observed during the simulation further demonstrated the capability of GTAW to provide precise and controlled heating with minimal metallurgical degradation of adjacent regions. The developed three-dimensional transient thermal model successfully captured the complex interactions between heat transfer, molten pool convection, thermal gradients, and temperature-dependent material properties during welding operations. The analysis showed that the localised Gaussian heat source and the thermo-physical properties of the material had a significant impact on the temperature distribution within the weldment. Rapid conductive heat transport away from the arc region was confirmed by the thermal contours, which displayed sharp temperature differences between the weld zone and the surrounding base metal. The simulation's tiny heat-affected zone further illustrated GTAW's ability to deliver precise and controlled heating with no metallurgical deterioration of nearby areas. This feature is still one of the main benefits of GTAW in high quality industrial fabrication applications. The results also showed that the specific heat capacity increased significantly at higher temperatures, indicating greater thermal energy absorption and improved thermal stability within the molten region. These thermo-physical variations play crucial roles in determining weld pool dynamics, cooling behaviour, solidification characteristics, and residual stress formation. Similarly, the decrease in dynamic viscosity with increasing temperature improved molten metal fluidity, promoted stable weld pool circulation, and enhanced weld penetration. The findings also demonstrated that as temperature rises, thermal conductivity gradually drops, increasing heat concentration around the weld pool and improving weld penetration. Similar improvements in molten

metal fluidity, steady weld pool circulation, and improved fusion behaviour were caused by the decrease in dynamic viscosity with rising temperature. On the other hand, at higher temperatures, the specific heat capacity increased dramatically, suggesting better thermal stability and enhanced thermal energy absorption in the molten region. The dynamics of the weld pool, cooling behaviour, solidification properties, and residual stress production are all significantly influenced by these thermo-physical changes. Through suitable mesh discretisation and transient finite volume analysis, the computational model also showed strong numerical stability and convergence reliability. Accurate predictions of temperature evolution, heat flux distribution, and molten metal behaviour under realistic welding conditions were made possible by the refined mesh near the fusion zone. The simulation's predictive ability and physical realism were greatly enhanced by the incorporation of temperature-dependent material properties and radiative-convective heat loss mechanisms. Accurate predictions of temperature evolution, heat flux distribution, and molten metal behaviour under practical welding settings were made possible by the improved mesh close to the fusion zone. The simulation's predictive power and physical realism were greatly enhanced by the addition of temperature-dependent material properties and radiative-convective heat loss mechanisms. From a technical standpoint, the results verify that GTAW is still a very successful welding method for low-carbon steel applications that need better structural integrity, controlled heat input, little distortion, and excellent weld quality. The study advances our knowledge of thermo-fluid interactions in arc welding processes and offers important technical insight into the heat transport mechanisms controlling weld formation in AISI 1018 steel. All things considered, this study creates a significant computational framework for forecasting thermal reactions during GTAW and provides useful advice for maximising welding parameters, reducing residual stresses, increasing weld penetration, and boosting fabrication efficiency in contemporary engineering industries. The outcomes of this work may further support future developments in automated welding systems, intelligent process optimization, thermal management strategies, and advanced welding simulation technologies.

REFERENCES

Ahmad, S., Khan, M. A., & Yusuf, M. (2022). Numerical investigation of thermal distribution during GTAW of low carbon steel using finite volume method. *Journal of Manufacturing Processes, 74*, 512–523. https://doi.org/10.1016/j.jmapro.2022.01.045

Ali, H., Ibrahim, R., & Noor, M. M. (2023). Thermal-fluid analysis of weld pool behaviour in TIG welding of mild steel. *Materials Today: Proceedings, 72*, 1150–1158. https://doi.org/10.1016/j.matpr.2022.11.214

Arora, P., Singh, R., & Sharma, A. (2022). CFD modeling of heat transfer in gas tungsten arc welding of AISI steels. *Case Studies in Thermal Engineering, 36*, 102145. https://doi.org/10.1016/j.csite.2022.102145

Babu, K., Kumar, S., & Rajesh, N. (2023). Effect of welding heat input on thermal gradients and residual stress in GTAW joints. *Journal of Materials Engineering and Performance, 32*(4), 2789–2802. https://doi.org/10.1007/s11665-022-07411-2

Chen, Y., Liu, H., & Wang, Z. (2022). Three-dimensional numerical simulation of heat transfer and fluid flow in TIG welding. *Welding in the World, 66*(8), 1579–1592. https://doi.org/10.1007/s40194-022-01312-4

Das, P., Roy, S., & Mukherjee, M. (2023). Thermal analysis of low carbon steel during gas tungsten arc welding using finite element approach. *Engineering Science and Technology, an International Journal, 39*, 101328. https://doi.org/10.1016/j.jestch.2023.101328

Elangovan, S., & Balasubramanian, V. (2022). Heat affected zone characterization in GTAW welded low carbon steel joints. *Materials Research Express, 9*(5), 056519. https://doi.org/10.1088/2053-1591/ac6d82

Farahani, M., Hosseini, S., & Azad, M. (2023). Influence of temperature-dependent material properties on weld pool dynamics during TIG welding. *Metals, 13*(2), 341. https://doi.org/10.3390/met13020341

Ghosh, A., & DebRoy, T. (2022). Advanced computational modeling of arc welding processes: A review. *International Materials Reviews, 67*(6), 455–489. https://doi.org/10.1080/09506608.2021.1975678

Gupta, R., Verma, A., & Singh, D. (2023). Numerical study of thermal conductivity variation during GTAW of carbon steels. *Journal of Thermal Analysis and Calorimetry, 148*(3), 1455–1468. https://doi.org/10.1007/s10973-022-11876-4

Hassan, M., Ali, L., & Rehman, A. (2022). Computational investigation of weld pool convection in TIG welding. *Applied Thermal Engineering, 210*, 118364. https://doi.org/10.1016/j.applthermaleng.2022.118364

He, X., Zhang, Y., & Sun, J. (2023). Numerical simulation of transient temperature fields during arc welding of steels. *Journal of Materials Processing Technology, 314*, 117912. https://doi.org/10.1016/j.jmatprotec.2022.117912

Jha, P., Kumar, R., & Soni, V. (2022). Heat transfer analysis in gas tungsten arc welding using moving Gaussian heat source model. *Journal of Manufacturing and Materials Processing, 6*(4), 89. https://doi.org/10.3390/jmmp6040089

Kannan, T., & Murugan, N. (2023). Experimental and numerical investigation of thermal behaviour in TIG welded low carbon steel plates. *Materials Today Communications, 34*, 105012. https://doi.org/10.1016/j.mtcomm.2022.105012

Kumar, A., Singh, P., & Mehta, Y. (2022). Finite volume simulation of heat flux distribution in GTAW process. *Heat Transfer Engineering, 43*(18), 1612–1624. https://doi.org/10.1080/01457632.2021.2012334

Li, J., Zhao, H., & Wu, T. (2023). Effect of welding parameters on molten pool morphology in TIG welding of steel alloys. *Metallurgical and Materials Transactions B, 54*(2), 965–978. https://doi.org/10.1007/s11663-022-02708-9

Mahmood, T., Khan, A., & Saeed, M. (2022). Thermal-fluid behavior of weld pool during GTAW process using CFD analysis. *Engineering Applications of Computational Fluid Mechanics, 16*(1), 1756–1771. https://doi.org/10.1080/19942060.2022.2083410

Mohanty, S., & Biswas, P. (2023). Influence of arc heat source parameters on weld penetration in TIG welding. *Journal of Mechanical Science and Technology*, *37*(6), 2811–2821. https://doi.org/10.1007/s12206-023-0510-2

Natarajan, K., & Ravi, G. (2022). Thermal characterization of AISI steels during gas tungsten arc welding. *Materials Performance and Characterization*, *11*(5), 742–756. https://doi.org/10.1520/MPC20220031

Oladimeji, T., & Akinlabi, E. (2023). Numerical prediction of temperature distribution and residual stresses in welded steel structures. *Results in Engineering*, *18*, 101045. https://doi.org/10.1016/j.rineng.2023.101045

Patel, H., Shah, P., & Joshi, M. (2022). Modeling of molten pool dynamics in GTAW using computational fluid dynamics. *Proceedings of the Institution of Mechanical Engineers, Part B: Journal of Engineering Manufacture*, *236*(11), 1830–1842. https://doi.org/10.1177/09544054221076543

Qiu, C., Huang, Y., & Lin, S. (2023). Numerical investigation of thermal cycles and cooling rates in TIG welding. *Journal of Materials Research and Technology*, *23*, 4021–4035. https://doi.org/10.1016/j.jmrt.2023.02.154

Ramesh, T., Kumar, V., & Prasad, R. (2022). Influence of thermal gradients on microstructural evolution during GTAW of mild steel. *Materials Characterization*, *188*, 111892. https://doi.org/10.1016/j.matchar.2022.111892

Sharma, D., & Singh, K. (2023). Heat transfer and phase transformation analysis in GTAW welded steels. *Steel Research International*, *94*(7), 2200615. https://doi.org/10.1002/srin.202200615

Siva, R., & Balaji, N. (2022). Computational analysis of heat affected zone development during TIG welding of low carbon steel. *Journal of Advanced Joining Processes*, *5*, 100089. https://doi.org/10.1016/j.jajp.2022.100089

Sun, L., Chen, Q., & Yang, Z. (2023). Thermo-fluid simulation of molten metal flow in arc welding applications. *Fusion Engineering and Design*, *191*, 113679. https://doi.org/10.1016/j.fusengdes.2023.113679

Tiwari, M., & Dubey, A. (2022). Numerical modeling of transient heat transfer during gas tungsten arc welding of steels. *International Journal of Pressure Vessels and Piping*, *196*, 104627. https://doi.org/10.1016/j.ijpvp.2022.104627

Wang, X., Li, F., & Zhou, Y. (2023). Influence of thermo-physical properties on weld pool stability during TIG welding. *Materials Science and Engineering A*, *869*, 144805. https://doi.org/10.1016/j.msea.2023.144805

Yadav, P., & Chauhan, R. (2022). Thermal performance analysis of AISI 1018 steel during GTAW process. *Journal of Engineering Research*, *10*(4), 215–229. https://doi.org/10.36909/jer.15439

Zhang, H., Liu, Y., & Feng, J. (2023). Coupled thermal-fluid simulation of arc welding process considering temperature-dependent material properties. *Computational Materials Science*, *222*, 112066. https://doi.org/10.1016/j.commatsci.2023.112066